

Finger-actuated, self-contained immunoassay cassettes

Xianbo Qiu · Jason A. Thompson · Zongyuan Chen · Changchun Liu · Dafeng Chen ·
Sudhir Ramprasad · Michael G. Mauk · Serge Ongagna · Cheryl Barber ·
William R. Abrams · Daniel Malamud · Paul L. A. M. Corstjens · Haim H. Bau

Published online: 14 July 2009

© Springer Science + Business Media, LLC 2009

Abstract The building blocks for an inexpensive, disposable, luminescence-based microfluidic immunoassay cassette are described, and their integration in a point-of-care diagnostic system is demonstrated. Fluid motion in the cassette is driven by depressing finger-actuated pouches. All reagents needed for the immunoassay can be stored in the cassette in liquid form. Prior to use, the cassette consists of

two separate parts. A top storage component contains pouches, sealed storage chambers, a metering chamber, and needle seats. The bottom processing component contains connection needles, a mixing chamber, and a detection chamber with immobilized proteins. Subsequent to sample introduction, the storage and processing components are mated. The needles form hydraulic connections between the two parts and, in some cases, close valves. The pouches are then actuated sequentially to induce flow of various reagents and facilitate process operations. The cassette is compatible with different detection modalities. Both a cassette with immunochromatographic-based detection and a cassette with microbead-based detection were constructed and evaluated. The immunochromatographic cassette was used to detect antibodies to HIV in saliva samples. The bead-based cassette was used to detect the proinflammatory chemokine IL-8. The experimental data demonstrates good repeatability and reasonable sensitivity.

X. Qiu · J. A. Thompson · Z. Chen · C. Liu · D. Chen ·
S. Ramprasad · M. G. Mauk · H. H. Bau (✉)
Department of Mechanical Engineering and Applied Mechanics,
University of Pennsylvania,
Philadelphia, PA 19104, USA
e-mail: bau@seas.upenn.edu

S. Ongagna · C. Barber · W. R. Abrams · D. Malamud
Department of Basic Sciences,
New York University College of Dentistry,
New York 10010, USA

D. Malamud
Department of Medicine, NYU School of Medicine,
New York 10010, USA

P. L. A. M. Corstjens
Department of Molecular Cell Biology,
Leiden University Medical Center,
Leiden, The Netherlands

Present Address:
Z. Chen
Rheonix, Inc.,
22 Thornwood Dr.,
Ithaca, NY 14850, USA

Present Address:
S. Ramprasad
Pacific Northwest National Laboratory,
1000 NE Circle Blvd.,
Corvallis, OR 97330, USA

Keywords Microfluidic · Finger-actuation · Pouch ·
Needle · Immunoassay · Consecutive flow ·
Immunochromatography · Functionalized microbead array

1 Introduction

In recent years, there has been a growing interest in inexpensive, self-contained diagnostic devices for use at the point-of-care, at home, and in resource-poor regions of the world, where sophisticated laboratory services are not readily available (Kim et al. 2006; Wang et al. 2006; Li et al. 2005; Ho 2006; Ramachandran et al. 2006; Lim and Zhang 2007; Chen et al. 2007; Bhattacharyya and Klapperich 2007; Mauk et al. 2007). Although home care tests such as dip-sticks and lateral flow immunochromato-

graphic devices are widely available, they require the user to follow specific instructions and apply and blend reagents in a prescribed manner. This renders the tests practical only for relatively simple operations, and susceptible to both operator error and reagent contamination (Cardy and Allen 2004; Wilkinson et al. 2003). To increase test robustness, it is desirable to minimize the user's involvement in performing process operations. Microfluidics facilitates process automation and a reduction in operator involvement.

Microfluidic platforms for automated sample processing require both micropumps and microvalves to control the flow (Haeberle and Zengerle 2007), and microstirrers to enhance mixing of reagents. Throughout the years, various types of micropumps, such as piezoelectric, pneumatic, electrokinetic, and electrochemical, and numerous types of microvalves, including thermopneumatic, hydrogel, pneumatic, phase change, and membrane-based, have been developed (Zhang et al. 2007; Gu et al. 2004; Pilarski et al. 2005). Microstirrers used in microfluidics are typically classified as passive, when the energy needed for stirring is drawn from the pressure gradient that drives the flow (Hashimoto et al. 2006; Anderson et al. 2000), and active when another source of energy is used to facilitate stirring (Lee et al. 2005; Bau et al. 2001). In many cases, these components require silicon-based fabrication technology, are expensive to produce in small and moderate quantities, and are difficult to package. In this report we describe a polymer-based manufacturing technique that allows production of relatively inexpensive, integrated pumps, valves, and mixing elements that are fabricated together as part of the cassette. We rely on air or liquid filled, finger-actuated pouches to provide the pressure needed to drive the flow and on membrane-based valves to block certain flow passages.

Proteins are often detected with either sandwich (Qian and Bau 2003) or competitive (Qian and Bau 2004) immunoassays. Briefly, antibodies and/or antigens to specific target proteins are immobilized at a capture site. The sample mixed with diluent is brought into contact with the immobilized proteins to facilitate the binding of target analytes to the immobilized proteins. This is followed with a wash step to remove unbound material. Next, labels functionalized with secondary antibodies flow through the capture site to bind with the now immobilized target proteins. Finally, the unbound label is washed away. When high sensitivity is not required, the presence of the labels can be visually detected. When higher sensitivity is needed, one typically employs electronic transducers. In the case of optical detection, the labels are excited with a light source and their emission is detected with either a CCD camera or a photodiode (Caulum and Henry 2006). Typically, there is a difference between the excitation and emission wavelengths (Stokes shift), allowing one to discriminate

between the absorption and emission spectra with the use of appropriate filters. In our work, we used both fluorescent labels (AlexaFluor 488) and upconverting phosphor particles (UCP). UCP avoids some of the difficulties associated with the fluorescent labels since they exhibit an anti-Stokes shift by converting low-energy, infrared (IR) excitation (~980 nm) to high-energy phosphorescence emission in the visible spectrum (~450 nm) (Hampl et al. 2001). The advantages of UCP reporters over fluorescent labels include the absence of background autofluorescence from biological and inorganic materials, long shelf-life, and excellent stability (no photobleaching) (Rijke et al. 2001; Corstjens et al. 2008; Chen et al. 2007). Their disadvantage is a relatively large size, which may adversely impact mass transfer and reaction kinetics.

Previously, our group reported a timer-actuated, disposable immunoassay cassette for the detection of molecular markers in oral fluids (Liu et al. 2009). Here, we report an alternative, finger-driven cassette, which does not require an external mechanical drive. Another difference between the cassette described previously (Liu et al. 2009) and the one presented here is the staging of mixing channels, the reagent storage chambers, and the reaction/processing chambers.

2 Cassette design

This section describes the modular components of the integrated, microfluidic cassette, which are generic and can be combined in various ways to build different types of integrated systems. For clarity, we focus on a specific immunochromatographic assay operating in a consecutive flow format (Corstjens et al. 2007). Later, we show how the same building blocks can be combined to facilitate highly multiplexed assays utilizing microbead arrays.

2.1 Overview

We describe here the use of a finger-actuated cassette to detect antibodies and antigens in oral fluids using the consecutive flow format (Malamud et al. 2005). Briefly, a sample of oral fluid is mixed with a diluent and transmitted to a nitrocellulose lateral flow strip. The strip contains a test zone consisting of immobilized, synthetic peptides of HIV envelope glycoproteins and a control line of immobilized goat anti-human IgG. Subsequently, the lateral flow strip is washed to remove unbound and non-specifically bound antibodies. Finally, UCP reporters functionalized with protein-A are discharged onto the strip to immunolabel the captured antibodies in the test zone and the anti-human IgG in the control zone. The intensity of the emitted signals

from the labels in the test and capture zones are measured and their ratio (T/C) is used to determine the results of the test. When the intensity ratio is above a certain threshold determined by analysis of negative samples, the test result is considered positive.

The cassette consists of two separate parts when stored: a top storage component and a bottom processing component. The storage component houses pouches, reagent storage chambers, and needle seats. The processing component contains interconnecting needles, connecting conduits, and a mixing and detection chamber. Prior to mating, the storage component lies upside down on the processing unit, with the pouches aligned with preformed protection cavities. This arrangement prevents inadvertent actuation of the pouches during shipment and storage.

The two parts of the cassette were fabricated with a computer numerical controlled (CNC) milling machine during the prototype development stage. The storage component was fashioned from high-density polyethylene since it can readily be thermally bonded with a flexible pouch matrix. The processing component was machined from polycarbonate due to its optical clarity (easing flow visualization) and better machinability, which allowed production of good quality needles and high definition conduits. However, it is anticipated that the two components will be made by injection molding for large scale production.

Once the sample is introduced into the storage component, a protective sealing layer is removed and the storage component is pressed against the processing component. The two components are aligned with positioning pins (Fig. 1(a)) and during mating, the needles protruding from the upper side of the processing component (Fig. 1(b)) penetrate into the storage component to form leak-free, fluidic connections between the two parts. In addition to completing fluidic circuits, some of the needles have the dual role of closing flow passages upon penetration.

2.2 Pouch-based actuation

To facilitate simplicity and portability, we used pouches as a pressure source for fluid flow. The fabrication process for the pouches is depicted schematically in Fig. 2. First, pouch cavities were CNC-machined (Haas Milling OM-2A, Haas Automation Inc., Oxnard, CA) in the upper surface of the storage component with ball-end mills. The size of the cavities was determined by the pouch volume required during operation. Second, a thin ($\sim 100\mu\text{m}$) barrier film (TPS-4049B, Tolas Inc., Feasterville, PA) was thermally bonded to the surface of the polyethylene (Product #8619K451, McMaster-Carr, Princeton, NJ) with a thermal bonding press (Hydraulic Unit #3912, Carver Inc., Wabash, IN) at 135°C with a force of ~ 150 lbs for 5 sec.

Third, the thin film was deformed with a solid metal ball at room temperature until the membrane made contact with the bottom of the pouch cavity. Finally, air pressure was applied through an access hole at the base of the cavity to inflate the pouch into a hemisphere-like dome above the surface (Fig. 2(d)). Once depressed during operation, the pouch remains in the deformed state (Fig. 2(c)). This characteristic proved useful to prevent backflow of the discharged fluids. Although the pouches can either be filled with liquid or with air, ultimately air-filled pouches (pneumatic drive) were selected for the immunochromatographic cassette to reduce dead volumes (less than 5%).

In a typical operation, once the storage and processing components had been mated (Fig. 1(a)), a connection is formed between the pouch and the reagent storage chamber. Upon compressing the pouch, the air discharged from the pouch displaces the reagents from the storage chamber into the channel. Several alternative design options for pouch actuation include a microprocessor-controlled electric motor, a spring-wound timer mechanism (Liu et al. 2009), or manually. The last design option is reported here.

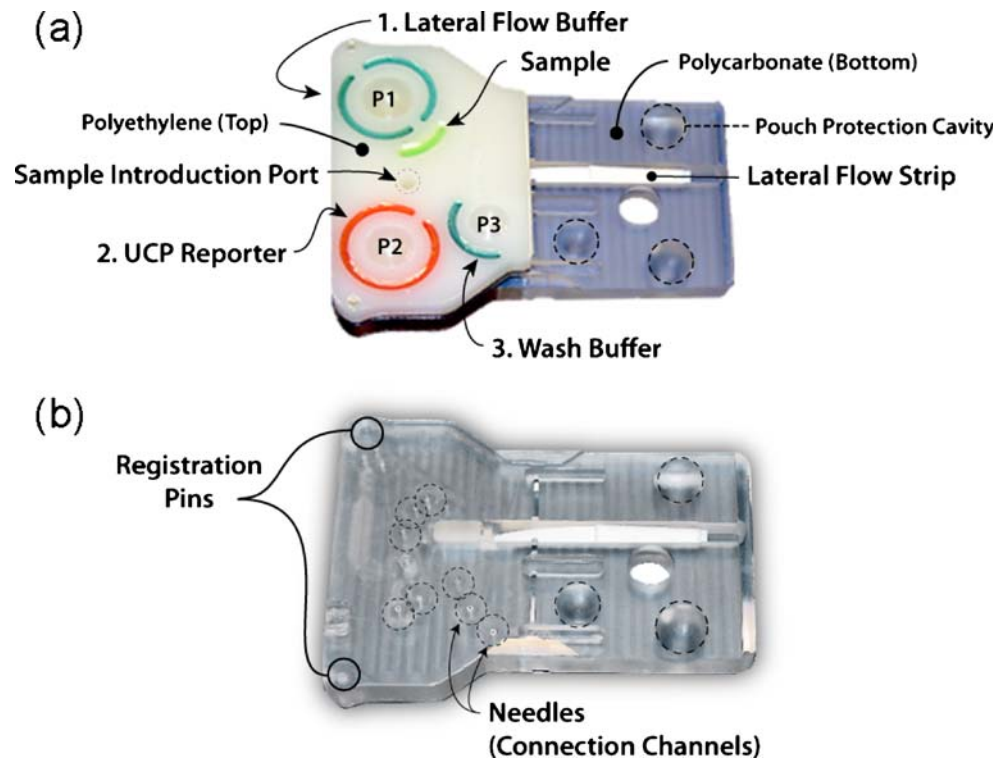
2.3 Seal layer

Pressure sensitive, double-sided adhesive tape (Tape 9731, 3M, St. Paul, MN) forms the underside of the cassette storage component. Prior to attachment of the tape to the component, holes were cut in the tape with a CO_2 laser (Universal Laser Systems, Scottsdale, AZ) to accommodate the needles described in the next section. After the filling of the storage chambers with reagents, the underside of the storage component was sealed with aluminum foil (Microseal 'F' film, Bio-Rad Laboratories, Hercules, CA) to provide extended shelf life of the pre-stored reagents. Figure 3(a) depicts a cross-section of the storage component prior to mating, showing the double-sided adhesive tape with one protective layer and the aluminum sealing foil. Subsequent to sample introduction, the tape's protective layer and the aluminum foil are concurrently peeled off and the storage component is mated with the processing component.

2.4 Needle design, fabrication, and function

A robust microfluidic system requires easily produced, leakage-free, low dead-volume quick-connections (Snakenborg et al. 2007). Researchers have used micromachined needles for drug delivery, blood diagnosis, glucose monitoring, and cellular injection (Paik et al. 2004; Gardeniers et al. 2003; Kim and Lee 2007). For this device, needles are used to form connections between the two parts of the cassette (Fig. 3(b)). Figure 3(c) illustrates schematically

Fig. 1 (a) The assembled cassette ready to perform an immunoassay test. The polyethylene storage (top) component is shown mated with the polycarbonate processing (bottom) component. Air-filled pouches P1, P2, and P3 in the storage component dispense lateral flow buffer and sample, UCP reporter, and wash buffer, respectively. (b) The processing component of the cassette, illustrating the position of registration pins and interconnecting needles that facilitate the mating of the two components



the connection formed by the needles when the storage and processing components are mated. The needles and other processing components (Fig. 1(b)) were fabricated in polycarbonate (Product #8574K28, McMaster-Carr, Princeton, NJ).

A photograph of the needle (I.D.: 500 μm , wall thickness: 300 μm , height: 900 μm) is shown in Fig. 3(b) (inset). The needle has a flat head to assist in sealing and to facilitate valve actuation. The underside of the storage component consists of laser-cut, perforated, double-sided tape where the perforations match the positions of the needles (Fig. 3(a)). When the storage component is pressed against the processing component, the needle penetrates the perforated tape to form a leak-free connection between the two components through the needle's bore.

2.5 Single action valve and its actuation

The cassette is equipped with a metering chamber to facilitate semi-quantitative detection. A pipette tip is used to fill the metering chamber through a sample inlet port on the exterior of the cassette. Excess sample discharges into the waste chamber. During subsequent operations, the metering chamber is isolated from the inlet port on one side and from the waste chamber on the opposite side with passive, single-action valves. During the mating process, as the needles penetrate into the underside of the storage component, they close the passage between the sample introduction port and the metering chamber and the passage between the metering chamber and the waste chamber. At the same time, the needle upstream provides a connection

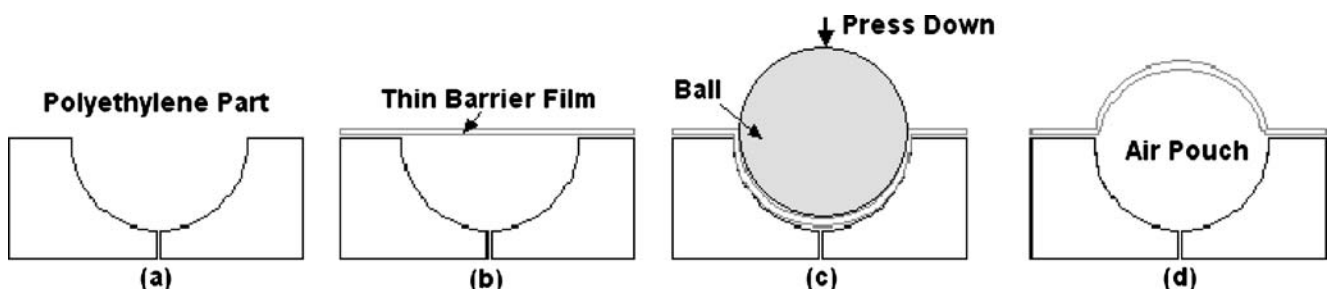


Fig. 2 The fabrication process for a pouch: (a) milling the pouch cavity; (b) bonding a thin film to the surface of the polyethylene; (c) deforming the thin film with a rigid ball; and (d) inflating the pouch with back pressure

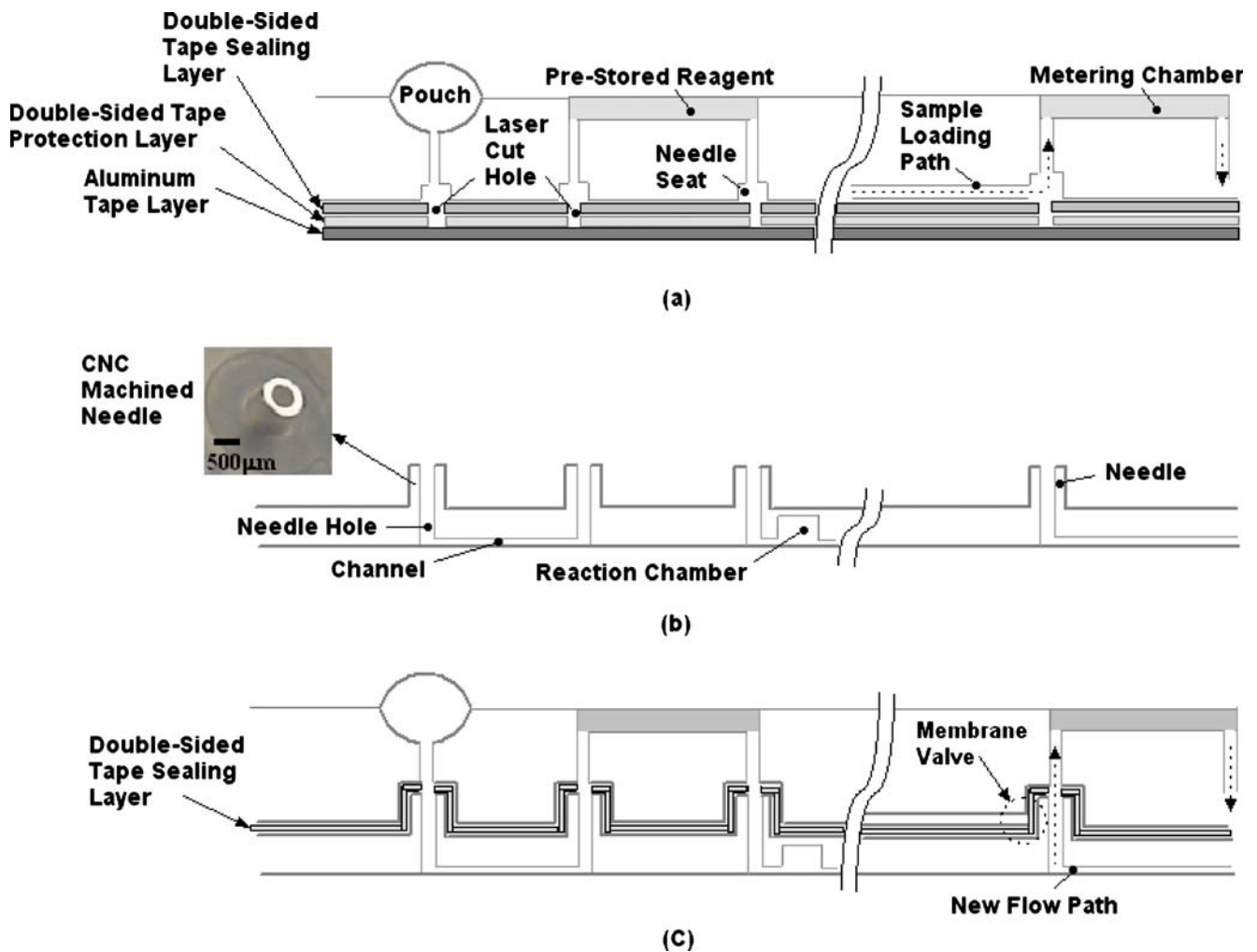


Fig. 3 Various cross-sections of the cassette. **(a)** The cassette's storage component. The layer of aluminum tape at the base of the component isolates the stored reagents from the outside environment. **(b)** The cassette's processing component. The needles interface with

their corresponding needle seats in **(a)** to form a leak-free connection between the storage and processing components of the cassette. Some of the needles also function to actuate one-time valves. **(c)** The assembled cassette

between a chamber upstream and the metering chamber. The needle downstream provides a connection between the metering chamber and a storage chamber downstream (Fig. 3(c)).

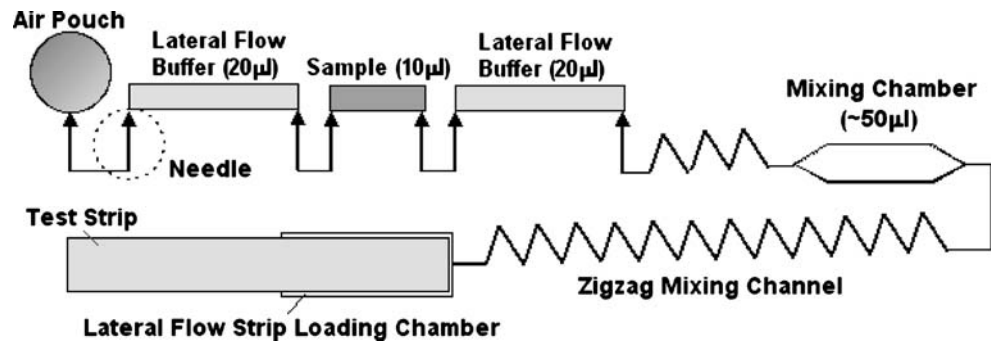
2.6 Mixing chamber

The immunoassay protocol calls for the mixing of the sample with diluent. Here, we employ a passive, zigzag mixer of the type used previously (Liu et al. 2009). The main difference between the previous and current embodiments is that previously sample and diluent were simultaneously introduced into the mixer using two pouches, while here we wish to facilitate manual operation which does not require synchronized, multi-pouch actuation. The metering chamber is positioned between two chambers containing diluent buffer. When the storage and processing compo-

nents are mated, connections are formed between the air pouch upstream, the lateral flow storage chamber, the sample metering chamber, the second lateral flow chamber downstream, and the mixing chamber (Fig. 4). Upon compressing the pouch, the contents of the three chambers flow into the mixing chamber, which provides a relatively large cross-section for primary mixing of the liquid slugs previously separated by trapped air pockets (of $\sim 1 \mu\text{L}$). The air discharged from the pouch displaces the mixture through the zigzag conduit downstream to the lateral flow strip. The bends in the zigzag conduit induce secondary flows (Yi and Bau 2003), which enhance mixing. The discharge speed is controlled by adjusting the size and hydraulic resistance of the flow passages.

To assess the efficiency of the serial-type zigzag mixer, we replaced the sample with rhodamine 123 fluorescent dye (Sigma-Aldrich, St. Louis, MO) with a 490 nm excitation

Fig. 4 The module for mixing the sample with lateral flow buffer and propelling the solution onto the lateral flow test strip



wavelength and 530 nm emission wavelength. The outlet of the zigzag channel was monitored with an epifluorescence microscope (BX51, Olympus Corporation, Melville, NY) equipped with a CCD camera (pco1600, Cooke Corporation, Romulus, MI) and 100 W mercury discharge lamp. Once the pouch was depressed, the camera recorded sequential images, which were converted to corresponding intensity values with imaging software (Wright Cell Imaging Facility (WCIF) ImageJ 1.37a, National Institutes of Health, Bethesda, MD).

Experiments were carried out to evaluate the mixing effectiveness by eluting a dilution series of homogeneous dyes to correlate the emission intensity with dye concentration. The solutions were loaded into the buffer and sample chambers, eluted through the mixer, and the elution emission intensity was recorded as a function of time. Figure 5 depicts an example of the elution emission intensity for three different cases: (a) 50 μL of stock fluorescent dye was loaded into the buffer and sample chambers; (b) 25 μL of stock fluorescent dye was pre-mixed with 25 μL of buffer and loaded into the buffer and sample chambers; and (c) 20 μL of buffer was loaded into the

upstream buffer chamber, 10 μL of stock fluorescent dye was loaded into the sample chamber, and 20 μL of buffer was loaded into the downstream buffer chamber. In all cases, once the solution left the detection region, the signal intensity rapidly declined back to a low, background level.

The variation in the flow rate accounted for the slight differences in the length of the high emission signal interval. In cases (a), (b), and (c), we recorded average emission intensities above the background of 11000, 6700, and 3700 units with corresponding standard deviations of 207, 390, and 280 units. The emission intensity can be approximately correlated with the concentration using the formula $\varphi I_0(1-\exp(-\epsilon bC))$, where φ is the quantum efficiency, I_0 is the incident radiant power, ϵ is the molar absorptivity, and b is the path length (Guilbault 1990). Based on the experimental emission intensities and the concentration in case (a) $C = C_0$ and in case (b) $C = C_0/2$, we estimate the concentration in case (c) as $C_0/4$, which is slightly above the actual mixed concentration. The fact that the standard deviation in (c) is comparable with (a) and (b) indicates that the mixer operates effectively and that the elution was well-mixed and nearly uniform in composition. The test was repeated several times with similar results.

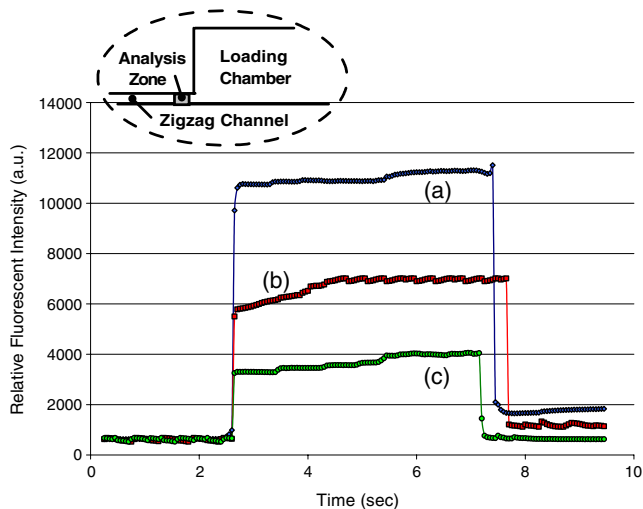


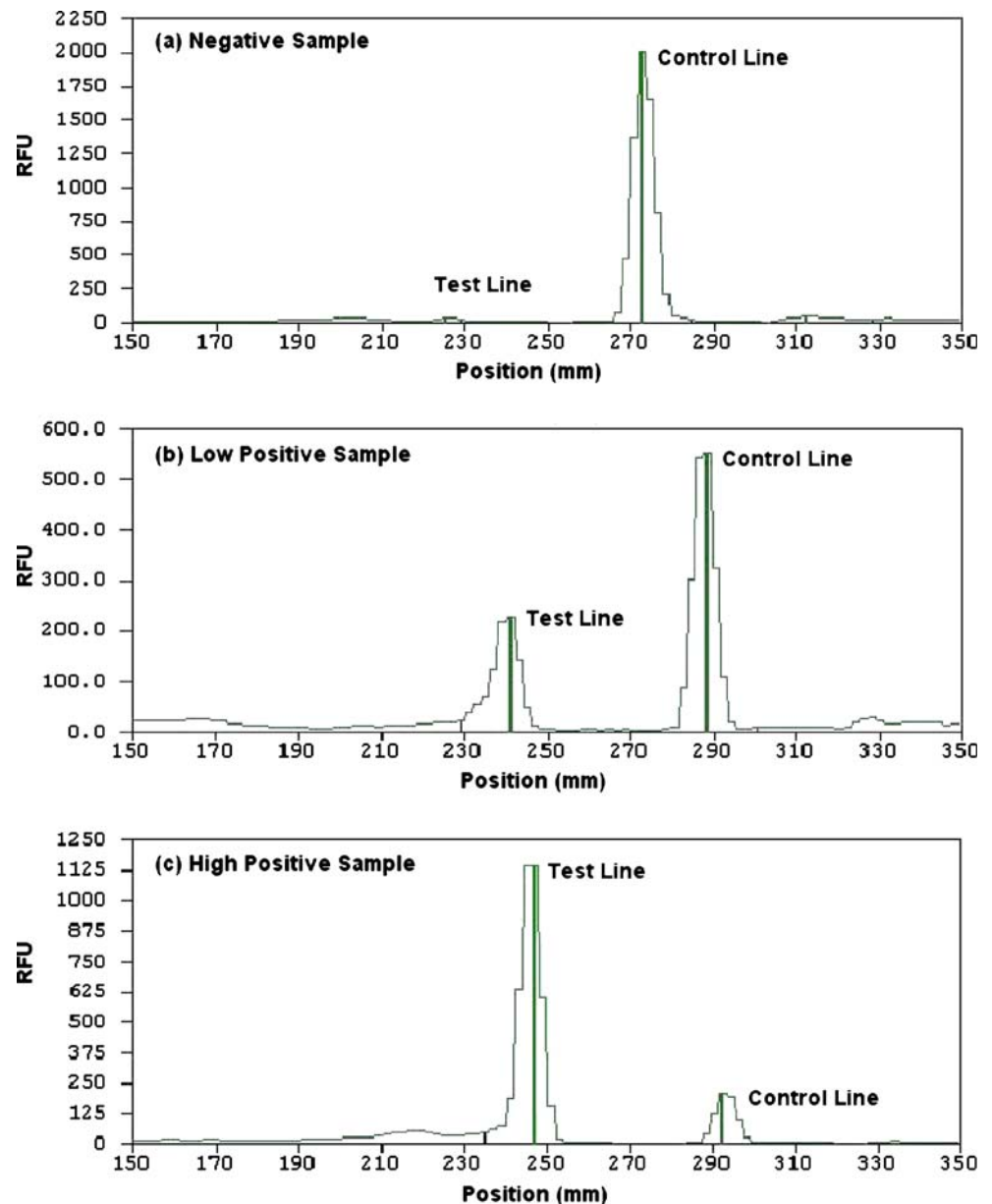
Fig. 5 Relative fluorescent intensity measurements as a function of time at the exit of the zigzag mixer. The emission intensity is illustrated for stock fluorescent dye (a), diluted dye (b), and fluorescent “sample” mixed with buffer (c)

3 Immunochromatographic assays

The consecutive flow immunoassay protocol consisted of three steps: (i) 10 μL of sample was mixed with 40 μL of lateral flow (LF) buffer (segmented into two portions of 20 μL upstream and 20 μL downstream of the sample), then blotted onto the lateral flow strip; (ii) after two minutes, 20 μL of LF buffer was blotted onto the strip to wash any unbound analytes; and (iii) two minutes later, 80 μL of LF buffer with 100 ng of UCP conjugate were added to the LF strip to label the immunoassay. After about fifteen minutes of incubation, the signals from the test and control lines were read with a Packard FluoroCount (Packard Instrument Company Inc., Meriden, CT).

The lateral flow buffer consisted of 100 mM Hepes (pH 7.2), 270 mM NaCl, 0.5% (v/v) Tween-20, and 1% (w/v) BSA (Sigma #7030A). The immuno-labeling buffer was a

Fig. 6 Laser scans of lateral flow test strips used for detecting the presence of HIV antibodies in saliva samples. The detected signal intensity is depicted as a function of position along the lateral flow strip for (a) negative; (b) low positive; and (c) high positive samples



mixture of LF buffer with protein-A coated UCP reporter particles. The HIV test LF strips were supplied by OraSure (OraSure Technologies Inc., Bethlehem, PA) and were constructed from nitrocellulose (20 mm, SRHF04000, Millipore, Billerica, MA) with a sample loading pad (10 mm, glass-fiber No. 33, Schleicher & Schuell, Maidstone, England) at the upstream end and an absorbent pad (20 mm, paper No. 470, Schleicher & Schuell) at the downstream end. The nitrocellulose of the HIV test LF strip had a test line consisting of HIV-specific antigens and a control line functionalized with anti-human IgG. The purpose of the control line was to bind the protein-A functionalized UCP labels to verify the successful migration of the labels up the strip.

HIV antibodies were spiked into clarified stimulated whole saliva obtained from consenting volunteers. The OraSure OraQuick ADVANCE Rapid HIV-1/2 Antibody Test Kit control was spiked into saliva to form the negative and low positive HIV samples. The high HIV positive sample was formulated by spiking serum from a Women's Interagency HIV Study (WIHS) subject with a high antibody titer into saliva.

Following incubation, the lateral flow strip was inserted into the Packard reader and the relative intensity of the UCP measured. Figure 6 depicts the fluorescence intensity of the negative, low positive, and high positive HIV samples in relative fluorescent units (RFU) as functions of position along the strip. The areas under the peaks are

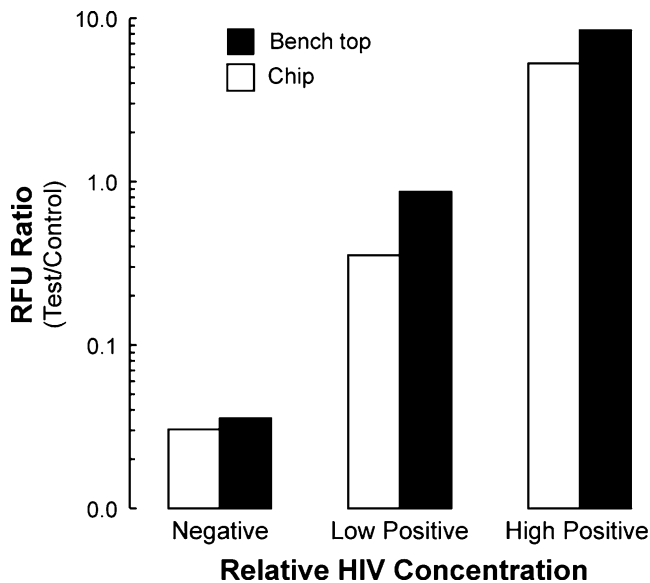


Fig. 7 Test/Control ratios of different samples of HIV antibodies

proportional to the amount of target analyte. The letters T and C, denote respectively the areas under the test and control peaks. The negative signal yielded no test peak and a large control peak. The low positive sample yielded moderately high test and control peaks. The high positive sample yielded a high test peak and a low control peak. The tests were repeated several times with similar results.

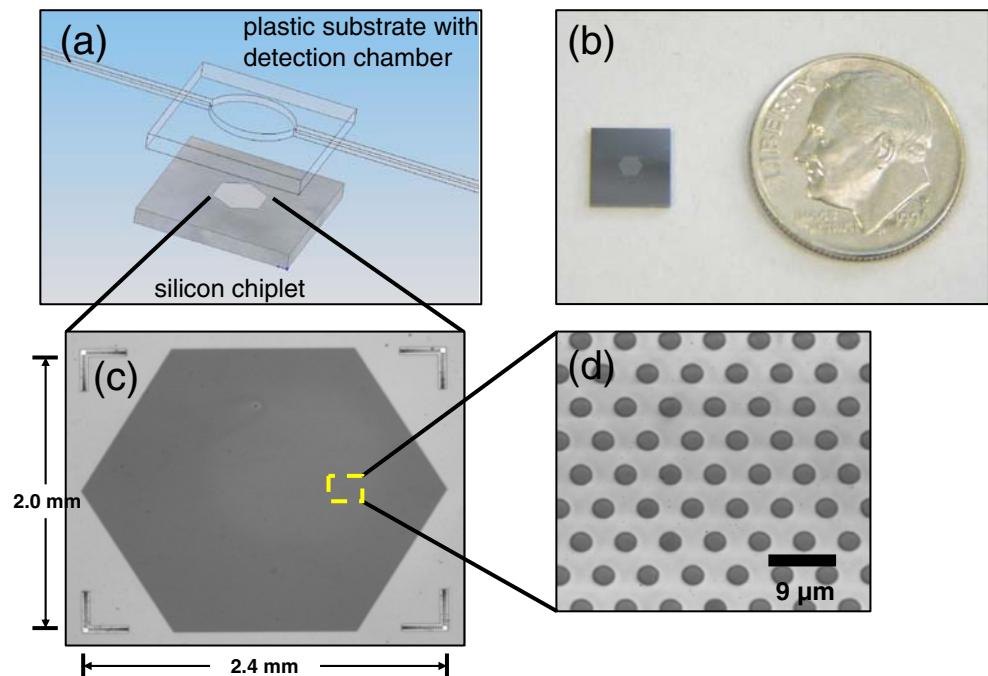
Figure 7 depicts the ratios (T/C) of the areas of the test and the control signals for both the cassette test and the benchtop test. The results shown here are based on an

earlier cassette design which utilized a microfluidic magnetic bar inside the mixing chamber instead of a zigzag mixing channel (see Fig. 4). However, to make the device entirely manually actuated, we replaced the magnetic stirrer with a passive zigzag mixer (Liu et al. 2009). Figure 7 shows that as the HIV antibody concentration increased, so did the T/C ratio. For the cassette, the T/C ratios of the negative, low positive and high positive samples were, respectively, 0.03, 0.35 and 5.28. For the benchtop, the T/C ratios of the negative, low positive and high positive samples were, respectively, 0.04, 0.87 and 8.43. The cassette exhibited a comparable performance to experiments conducted on the benchtop.

4 Microbead-based detection

To demonstrate that the cassette architecture can be used with other detection modalities, we constructed cassettes with integrated microbead arrays. Bead arrays are a powerful tool in the development of sensitive, multiplexed, on-chip, affinity assays (Ferguson et al. 2000; Goodey et al. 2001; Fan et al. 2006; Ng et al. 2008; Xu et al. 2008; Barbee and Huang 2008). Functionalized monodisperse microscopic beads were randomly, self-assembled into wells patterned on a silicon wafer (chiplet, Fig. 8) (Illumina Inc., San Diego, CA). After the microarray was loaded with beads from a master pool containing different bead types, the identification and location of each bead in the array was tabulated by means of a decoding process, whereby each bead type is identified either by its fluorescence intensity or

Fig. 8 The Illumina silicon chiplet containing a hexagon microbead array. (a) Schematic of the chiplet interfacing with the detection chamber milled in a plastic substrate. (b) Relative size of the chiplet. (c) Micrograph of the microarray of etched wells in the chiplet (20 \times). (d) Micrograph of a small region of the microarray showing individual empty wells (1000 \times); after loading, some of the wells are populated with functionalized beads



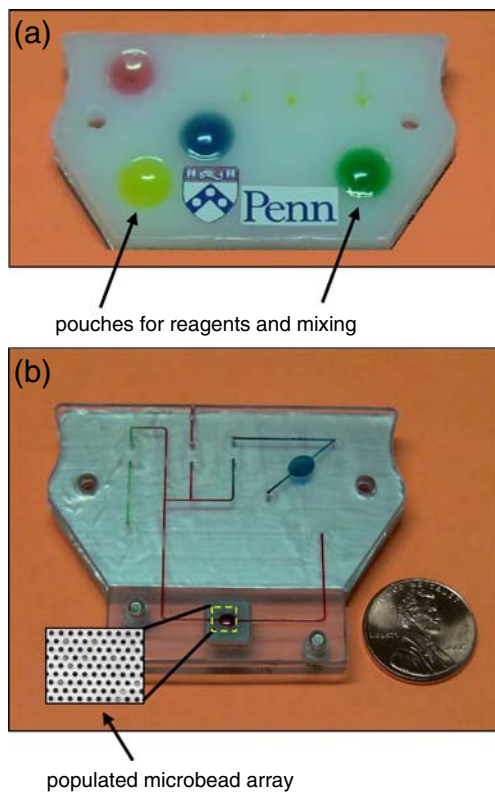


Fig. 9 Components of the lab-on-chip cassette for microbead immunoassays. **(a)** Polyethylene cartridge containing membrane valves and depressible pouches for reagent delivery and mixing. **(b)** Bottom side of a mated cassette showing polycarbonate substrate containing conduits, detection chamber, and silicon microbead array. The array contains wells populated with functionalized beads; the channels interface with the pouches and valves in **(a)** through interconnecting needles

emission wavelength. The emitted light is measured with a CCD camera.

4.1 Integration of microbead array into pouch-based cassette

In this design (Fig. 9(a)), the liquid buffers and wash solutions are stored directly in the hemispherical pouches (~50-100 μL in volume) in contrast to the system depicted in Fig. 1, where the pouches were filled with air and the

reagents were stored in adjacent chambers. The lower polycarbonate component contains the flow conduits, reaction chambers, microbead array (chiplet), and needles to facilitate hydraulic connections. Prior to use, the two parts are mated using alignment pins to ensure proper connections. Figure 9(b) shows the bottom side of a mated cassette and illustrates how the chiplet interfaces with the fluidic channel and detection chamber. The transparent cassette materials enable *in situ* imaging of the chiplet to determine the registry of target-specific beads according to their fluorescent coding and to detect the amount of specific target captured at each bead.

The pouch system utilized here facilitates easy, effective stirring. Two connected pouches—one initially empty and one full—work in tandem for mixing and incubation. As the full pouch is compressed, the empty pouch fills up; the process is then reversed, draining the full pouch into the empty receiving pouch. This reciprocating flow action enhances mass transfer and improves the reaction kinetics between target analytes, labels, and immobilized ligands. The stirrers provide an advantage over commonly used, commercially available microarrays, where interaction kinetics are governed mostly by diffusion.

4.2 Detection of IL-8 with cassette and microbead array

To demonstrate the utility of the cassette with the microbead array, we performed a bead-based fluorescence sandwich immunoassay. The microbeads and reagents for this assay were provided by Dr. David Walt at Tufts University. The steps associated with the assay are depicted in Fig. 10 (which is a modification of a figure presented in Blicharz et al. 2009). In the experiment, we used only two distinct bead types, however the assay can be readily extended to include many more beads to concurrently test for a large number of targets. The two model proteins used in this experiment were Interleukin-8 (IL-8, 8 kDa) and Vascular Endothelial Growth Factor (VEGF, 42 kDa).

An Illumina hexagon well array etched in silicon was loaded with a mixture of 3.1 μm diameter polymer beads (Bangs Laboratories Inc., Fishers, IN) coated with anti-IL-8 and anti-VEGF. The beads were impregnated with the

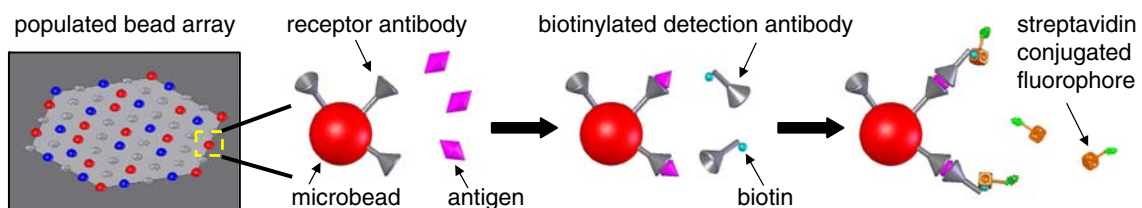


Fig. 10 A representative protein immunoassay. Two types of pre-encoded microbeads coated with different receptor antibodies (Blicharz et al. 2009) are immobilized in wells etched in silicon. Antigen is then

incubated with the array and binds its respective microbead. Next a biotinylated detection antibody is incubated with the array, and finally labeled with a streptavidin conjugated fluorescent reporter

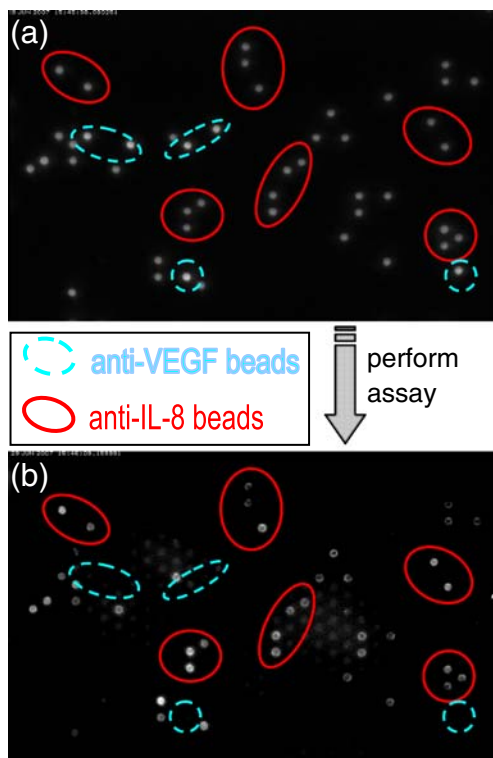


Fig. 11 Fluorescent micrographs from cassette protein assay with IL-8 target. **(a)** Encoding image (ex: 365 nm, em: 605 nm) of microbead array populated with anti-VEGF coated beads (more intense, dashed-circled in blue) and anti-IL-8 coated beads (less intense, several beads circled in red). **(b)** Signal image (ex: 495 nm, em: 519 nm) of same region of array taken subsequent to performing protein assay with IL-8 target. The target was specifically captured, as demonstrated by fluorescent emission from only the anti-IL-8 beads

fluorescent dye Europium III (ex: 365 nm, em: 605 nm) at different concentrations such that the anti-VEGF beads were brighter than the anti-IL-8 beads at a 605 nm emission wavelength. See Blicharz et al. (2009) for a description of the bead preparation procedure. The beads were dried on the array under room conditions and slight pressure was applied to the beads to assist settling. The excess beads were removed with a lint-free cloth soaked in Tris Buffered Saline (TBS) containing 0.05% Tween-20 wash solution. The loaded chiplet was mounted into the polycarbonate substrate containing $330 \times 330 \mu\text{m}^2$ square conduits and an ellipsoid-shaped detection chamber (long axis: 2.54 mm, short axis: 2.03 mm, depth: 380 μm) (Fig. 9(b)) and sealed with double-sided adhesive tape that had a laser-cut viewing window. In addition the chiplet was secured with a gasket and a bolted plate.

Biotinylated anti-IL-8 detection antibody (R&D Systems, Minneapolis, MN) was pre-mixed with the streptavidin AlexaFluor 488 fluorescent label (Invitrogen, Carlsbad, CA) such that the final solution contained a concentration of 3 $\mu\text{g}/\text{mL}$ antibody and 20 $\mu\text{g}/\text{mL}$ label. This solution was injected into a pouch in the polyethylene cartridge and

another pouch was filled with wash buffer (TBS + 0.05% Tween-20). After loading, the cartridge was sealed with a piece of double-sided adhesive aluminum foil (All-Foils Inc., Brooklyn Heights, OH).

To initiate the assay, the polyethylene cartridge was mated with the polycarbonate substrate, and an 125 nM IL-8 sample (R&D Systems, Minneapolis, MN) was injected into the cassette inlet port until it covered the bead array. A background image of the beads using an AlexaFluor 488 filter cube (ex: 495 nm, em: 519 nm) was taken to ensure that the beads did not autofluoresce. The sample was incubated on the array for 30 min at room temperature and the secondary antibody mixed with AlexaFluor 488 solution flowed over the array for 20 min with pouch mixing. Unbound constituents were washed away from the bead array into an empty pouch using the wash pouch. The encoding and signal images were captured using, respectively, Europium and AlexaFluor filter cubes (Chroma Technology Corporation, Rockingham, VT). Representative camera images are shown in Fig. 11. The encoding image (Fig. 11(a)) shows the location of the two bead types in the array, and the signal image (Fig. 11(b)) demonstrates that only the anti-IL-8 beads fluoresced at the label wavelength. This indicates that the IL-8 target was captured and labeled by the AlexaFluor 488 and that there was undetectable non-specific binding to the anti-VEGF beads.

5 Conclusions and outlook

Building blocks for an integrated, disposable, microfluidic cassette with on-board storage of reagents were developed, constructed, and successfully tested. The cassette consists of two components: a storage component and a processing component. During storage, the two components are disengaged. The two parts are mated immediately after sample loading. Hydraulic connections between the two parts are facilitated with needles that protrude from the processing component and penetrate into the storage component. The needles also can serve a secondary role as valve actuators that close flow passages that are no longer needed after sample introduction. The cassette can be actuated with mechanical actuators or manually via finger-actuation. The cassette architecture provides a flexible platform that can accommodate various detection modalities.

The utility of the cassette was demonstrated experimentally with two representative assays and two different means of detection. In the first instance, HIV antibodies in saliva samples were detected using a lateral flow strip. In the second case, the protein IL-8 was detected with an integrated microbead array. The lateral flow detection utilized UCP labels that have the unique property of a

negative Stokes shift which eliminates background emission. The bead array utilized more conventional fluorescent labels. For low sensitivity detection and with labels such as gold, the cassette with the lateral flow could possibly be used without an optical reader, thus providing an inexpensive, un-instrumented test, which can be deployed in resource poor regions of the world. For higher sensitivity and in the case of the bead array-based detection, one must employ a reader to capture the signal.

Acknowledgments The research was funded, in part, by National Institute of Health Grants U01-DE-017855 and U01-DE-017788, and National Science Foundation Integrative Graduate Education and Research Traineeship Program Grant DGE-0221664 to JAT. The samples used in this study were collected by the Women's Interagency HIV Study and its associated Collaborative Study Groups. Dr. David Walt's group at Tufts University provided the Illumina chiplet and the reagents and protocols to carry out the microbead array tests. Dr. Timothy Blicharz (a graduate of Walt's group) assisted with the microbead detection assay. Ms. Mian Qin provided insights into the mixing process in the cassette.

References

- R.C. Anderson, X. Su, G.J. Bogdan, J. Fenton, A miniature integrated device for automated multistep genetic assays. *Nucleic Acids Res.* **28**, i–vi (2000)
- K.D. Barbee, X. Huang, Magnetic assembly of high-density DNA arrays for genomic analyses. *Anal. Chem.* **80**, 2149–2154 (2008)
- H.H. Bau, J. Zhong, M. Yi, A minute magneto hydro dynamic (MHD) mixer. *Sens. Actuators B* **79**, 207–215 (2001)
- A. Bhattacharyya, C.M. Klapperich, Design and testing of a disposable microfluidic chemiluminescent immunoassay for disease biomarkers in human serum samples. *Biomedical Microdevices* **9**, 245–251 (2007)
- T.M. Blicharz, W.L. Siqueira, E.J. Helmerhorst, F.G. Oppenheim, P.J. Wexler, F.F. Little, D.R. Walt, Fiber-optic microsphere-based antibody array for the analysis of inflammatory cytokines in saliva. *Anal. Chem.* **81**, 2106–2114 (2009)
- D.L.N. Cardy, G.J. Allen, Lateral flow assay device and method, International Patent, Publication No.: WO/2004/007078
- M.M. Caulum, C.S. Henry, Multi-analyte immunoassay using cleavable tags and microchip micellar electrokinetic chromatography. *Analyst* **131**, 1091–1093 (2006)
- Z. Chen, M.G. Mauk, J. Wang, W.R. Abrams, P.L.A.M. Corstjens, R. S. Niedbala, D. Malamud, H.H. Bau, A microfluidic system for saliva-based detection of infectious diseases, *Ann. N.Y. Acad. Sci.* **1098**, 429–436 (2007)
- P.L.A.M. Corstjens, Z. Chen, M. Zuiderwijk, H.H. Bau, W.R. Abrams, D. Malamud, R.S. Niedbala, H.J. Tanke, Rapid assay format for multiplex detection of humoral immune responses to infectious disease pathogens (HIV, HCV, and TB). *Ann. N.Y. Acad. Sci.* **1098**, 437–445 (2007)
- P.L.A.M. Corstjens, M. Zuiderwijk, H.J. Tanke, J. van der Ploeg-Schip, T.H.M. Ottenhoff, A. Geluk, A user-friendly, highly sensitive assay to detect the IFN- γ secretion by T cells. *Clin. Biochem.* **6**, 440–444 (2008)
- J.B. Fan, K.L. Gunderson, M. Bibikova, J.M. Yeakley, J. Chen, E. Wickham Garcia, L.L. Lebruska, M. Laurent, R. Shen, D. Barker, Illumina universal bead arrays. *Methods Enzymol.* **410**, 57–73 (2006)
- J.A. Ferguson, F.J. Steemers, D.R. Walt, High-density fiber-optic DNA random microsphere array. *Anal. Chem.* **72**, 5618–5624 (2000)
- H.J.G.E. Gardeniers, R. Lutge, E.J.W. Berenschot, M.J. de Boer, S.Y. Yeshurun, M. Hefetz, R. van't Oever, A. van den Berg, Silicon micromachined hollow microneedles for transdermal liquid transport. *Journal of Microelectromechanical Systems* **6**, 855–862 (2003)
- A. Goodey, J.J. Lavigne, S.M. Savoy, M.D. Rodriguez, T. Curey, A. Tsao, G. Simmons, J. Wright, S. Yoo, Y. Sohn, E.V. Anslyn, J.B. Shear, D.P. Neikirk, J.T. McDevitt, Development of multianalyte sensor arrays composed of chemically derivatized polymeric microspheres localized in micromachined cavities. *J. Am. Chem. Soc.* **123**, 2559–2570 (2001)
- W. Gu, X. Zhu, N. Futai, B.S. Cho, S. Takayama, Computerized microfluidic cell culture using elastomeric channels and Braille displays. *PNAS* **45**, 15861–15866 (2004)
- G.G. Guilbault, Practical fluorescence, 2nd edition, CRC Press (ISBN 0824783506, 9780824783501) (1990)
- S. Haeberle, R. Zengerle, Microfluidic platforms for lab-on-a-chip applications. *Lab Chip* **7**, 1094–1110 (2007)
- J. Hampl, M. Hall, N.A. Muftic, Y.M. Yao, D.B. MacQueen, W.H. Wright, D.E. Cooper, Upconverting phosphor reporters in immunochromatographic assays. *Anal. Biochem.* **288**, 176–187 (2001)
- M. Hashimoto, F. Barany, S.A. Soper, Polymerase chain reaction/ligase detection reaction/hybridization assays using flow-through microfluidic devices for the detection of low-abundant DNA point mutations. *Biosens. Bioelectron.* **10**, 1915–1923 (2006)
- W.Z. Ho, Self-contained microfluidic biochip and apparatus, United States Patent, Patent No.: US 7122153 (2006)
- K. Kim, J.B. Lee, High aspect ratio tapered hollow metallic microneedle arrays with microfluidic interconnector. *Microsyst. Technol.* **13**, 231–235 (2007)
- D.S. Kim, S.H. Lee, C.H. Ahn, J.Y. Lee, T.H. Kwon, Disposable integrated microfluidic biochip for blood typing by plastic microinjection molding. *Lab Chip* **6**, 794–802 (2006)
- C.Y. Lee, G.B. Lee, J.L. Lin, F.C. Huang, C.S. Liao, Integrated microfluidic systems for cell lysis, mixing/pumping and DNA amplification. *J. Micromechanics Microengineering* **15**, 1215–1223 (2005)
- S. Li, P.N. Floriano, N. Christodoulides, D.Y. Fozdar, D. Shao, M.F. Ali, P. Dharshan, S. Mohanty, D. Neikirk, J.T. McDevitt, S. Chen, Disposable polydimethylsiloxane/silicon hybrid chips for protein detection. *Biosens. Bioelectron.* **21**, 574–580 (2005)
- C.T. Lim, Y. Zhang, Bead-based microfluidic immunoassays: the next generation. *Biosens. Bioelectron.* **22**, 1197–1204 (2007)
- C. Liu, X. Qiu, S. Ongagna, D. Chen, Z. Chen, W.R. Abrams, P.L. Corstjens, H.H. Bau, A timer-actuated immunoassay cassette for detecting molecular markers in oral fluids. *Lab Chip* **9**, 768–776 (2009)
- D. Malamud, H. Bau, S. Niedbala, P. Corstjens, Point detection of pathogens in oral samples. *Adv. Dent. Res.* **18**, 12–16 (2005)
- M.G. Mauk, B.L. Ziober, Z. Chen, J.A. Thompson, H.H. Bau, Lab-on-a-chip technologies for oral-based cancer screening and diagnostics: capabilities, issues, and prospects. *Ann. N.Y. Acad. Sci.* **1098**, 467–475 (2007)
- J.K. Ng, E.S. Selamat, W. Liu, A spatially addressable bead-based biosensor for simple and rapid DNA detection. *Biosens. Bioelectron.* **23**, 803–810 (2008)
- S.J. Paik, S. Byun, J.M. Lim, Y. Park, A. Lee, S. Chung, J. Chang, K. Chun, D. Cho, In-plane single-crystal-silicon microneedles for minimally invasive microfluid systems. *Sens. Actuators A* **114**, 276–284 (2004)
- P.M. Pilarski, S. Adamia, C.J. Backhouse, An adaptable microvalving system for on-chip polymerase chain reactions. *J. Immunol. Methods* **305**, 48–58 (2005)

- S. Qian, H.H. Bau, A mathematical model of lateral flow bio-reactions applied to sandwich assays. *Anal. Biochem.* **322**, 89–98 (2003)
- S. Qian, H.H. Bau, Analysis of lateral flow bio-detectors: competitive format. *Anal. Biochem.* **326**, 211–224 (2004)
- S. Ramachandran, J. Gerdes, P. Tarr, P. Yager, L. Dillman, R. Peck, M. Kokoris, M. Nabavi, F. Battrell, D. Hoekstra, B.H. Weigl, Dry-reagent storage for disposable lab-on-a-card diagnosis of enteric pathogens, Proceedings of the 1st Distributed Diagnosis and Home Healthcare (D2H2) Conference Arlington, 16–19 (2006)
- D. Snakenborg, G. Perozziello, O. Geschke, J.P. Kutter, A fast and reliable way to establish fluidic connections to planar microchips. *J. Micromechanics Microengineering* **17**, 98–103 (2007)
- F. van de Rijke, H. Zijlmans, S. Li, T. Vail, A.K. Raap, R.S. Niedbala, H.J. Tanke, Up-converting phosphor reporters for nucleic acid microarrays. *Nat. Biotechnol.* **19**, 273–276 (2001)
- J. Wang, Z. Chen, P.L.A.M. Corstjens, M.G. Mauk, H.H. Bau, A disposable microfluidic cassette for DNA amplification and detection. *Lab Chip* **6**, 46–53 (2006)
- R. Wilkinson, D. Rowland, W.M. Ching, Development of an improved rapid lateral flow assay for the detection of orientia tsutsugamushi-specific IgG/IgM antibodies. *Ann. N.Y. Acad. Sci.* **990**, 386–390 (2003)
- W. Xu, K. Sur, H. Zeng, A. Feinerman, D. Kelso, J.B. Ketterson, A microfluidic approach to assembling ordered microsphere arrays. *J. Micromechanics Microengineering* **18**, 1–6 (2008)
- M. Yi, H.H. Bau, The kinematics of bend-induced mixing in micro-conduits. *Int. J. Heat Fluid Flow* **24**, 645–656 (2003)
- C. Zhang, D. Xing, Y. Li, Micropumps, microvalves, and micromixers within PCR microfluidic chips: advances and trends. *Biotechnol. Adv.* **25**, 483–514 (2007)